NeuroImage 95 (2014) 193–207

Contents lists available at ScienceDirect

NeuroImage

journal homepage: www.elsevier.com/locate/ynimg

The development of human amygdala functional connectivity at rest from 4 to 23 years: A cross-sectional study

Laurel J. Gabard-Durnam [a,*], Jessica Flannery [a], Bonnie Goff [a], Dylan G. Gee [a], Kathryn L. Humphreys [a], Eva Telzer [b], Todd Hare [c], Nim Tottenham [a]

[a] University of California, Los Angeles, Department of Psychology, Los Angeles, CA 90095, USA
[b] University of Illinois at Urbana–Champaign, Department of Psychology, Champaign, IL 61820, USA
[c] University of Zurich, Department of Economics, Zurich, CH 8006, Switzerland

ARTICLE INFO

Article history:
Accepted 15 March 2014
Available online 21 March 2014

Keywords:
Amygdala
Amygdala subnuclei
Development
Medial pre-frontal cortex
Resting-state

ABSTRACT

Functional connections (FC) between the amygdala and cortical and subcortical regions underlie a range of affective and cognitive processes. Despite the central role amygdala networks have in these functions, the normative developmental emergence of FC between the amygdala and the rest of the brain is still largely undefined. This study employed amygdala subregion maps and resting-state functional magnetic resonance imaging to characterize the typical development of human amygdala FC from age 4 to 23 years old (n = 58). Amygdala FC with subcortical and limbic regions was largely stable across this developmental period. However, three cortical regions exhibited age-dependent changes in FC: amygdala FC with the medial prefrontal cortex (mPFC) increased with age, amygdala FC with a region including the insula and superior temporal sulcus decreased with age, and amygdala FC with a region encompassing the parahippocampal gyrus and posterior cingulate also decreased with age. The transition from childhood to adolescence (around age 10 years) marked an important change-point in the nature of amygdala–cortical FC. We distinguished unique developmental patterns of coupling for three amygdala subregions and found particularly robust convergence of FC for all subregions with the mPFC. These findings suggest that there are extensive changes in amygdala–cortical functional connectivity that emerge between childhood and adolescence.

Introduction

Activity of the amygdala and the associated cortex underlies emotional attention, learning, and regulation (Adolphs and Spezio, 2006; Ochsner et al., 2012; Phillips et al., 2003). A robust human neuroimaging literature has shown that it is the functional connections between regions in these networks that underlie these affective and cognitive processes (Hariri et al., 2003; Kim et al., 2011a; Ochsner et al., 2012), and the strength of these functional connections has predicted emotional behaviors of healthy adults (Banks et al., 2007; Lee et al., 2012). Furthermore, atypical functional connectivity patterns within these networks have been implicated in disrupted affective and cognitive processes in a range of clinical populations, including those with anxiety, depression, schizophrenia, and bipolar disorder (Anand et al., 2005; Berking and Wupperman, 2012; Cisler and Olatunji, 2012; Das et al., 2007; Henry et al., 2008; Wang et al., 2009). Intrinsic, "resting" activity is critical for maintaining the integrity of functional connections, accounting for the vast majority of the brain's energy expenditure, so resting-state functional magnetic resonance imaging (fMRI) indexing these connections is a powerful approach for understanding composition and stability of these functional networks (Raichle, 2010; Tomasi et al., 2013).

Importantly, studies assessing amygdala–cortical functional connectivity through both resting-state and task analyses have focused on mature networks in adults, while the development of these functional connections is yet largely uncharacterized. Dramatic changes occur across childhood and adolescence in emotional behaviors that have been associated with amygdala-mediated cortical functional connections (e.g., emotion processing tasks: Gee et al., 2013; Hare et al., 2008; Perlman and Pelphrey, 2011; emotion reappraisal: McRae et al., 2012). Notably, the human amygdala's early maturation and functionality in childhood (Gee et al., 2013; Gilmore et al., 2012; Swartz et al., 2014; Thomas et al., 2001; Ulfig et al., 2003), along with the late maturation and functional development of cortical regions that can extend into adulthood together delineate a vast age-range during which amygdala–cortical functional connections may develop (Bunge et al., 2002; Casey et al., 1997, 2000; Giedd et al., 1996; Gogtay et al., 2004;

* Corresponding author at: University of California, Los Angeles, 1285 Franz Hall, Room 1354, Los Angeles, CA 90095-1563, USA.
E-mail address: ljgabarddurnam@ucla.edu (L.J. Gabard-Durnam).

http://dx.doi.org/10.1016/j.neuroimage.2014.03.038
1053-8119/

Killgore and Yurgelun-Todd, 2004; Sowell et al., 2007). Qin et al. (2012) have recently noted weaker amygdala–cortical resting-state connectivity strengths in children (ages 7–9) compared to adults (ages 19–22). This paper was important because it showed that resting-state amygdala–cortical connectivity was different between children and adults. In the current study, we aimed to extend these findings by characterizing the timing and extent of changes in functional connectivity during development within the framework of a cross-sectional design. Characterizing the changes between early childhood and adulthood in these cortical and subcortical networks' construction can begin to inform how and when functional connections with the amygdala appear, delineate developmental transitions in these networks' construction, and identify periods of plasticity when these connections are sensitive to environmental influences (Sporns and Zwi, 2004).

We therefore assessed amygdala–cortical and subcortical functional connectivity development cross-sectionally from age 4–23 years using resting-state fMRI, which is ideal for participants spanning such a wide age-range (Pizoli et al., 2011; Uddin et al., 2010; Van Dijk et al., 2010). Specifically, we distinguished between age-controlled and age-dependent connectivity patterns with the amygdala. We anticipated that some regions would show mature connectivity with the amygdala by childhood, and sought to identify those regions that showed developmental change as well as quantify the timing, nature, and duration of these changes.

Secondly, while human studies have largely assessed connectivity with the amygdala as a homogenous structure, it is a complex of structurally and functionally distinct nuclei (Amaral et al., 1992; Amunts et al., 2005; LeDoux, 2003; Price, 2003). Initial studies using anatomical maps demonstrate the utility in differentiating these subregions in humans, finding both distinct activations and functional networks across subregions (Ball et al., 2007; Roy et al., 2009). Weaker segregation in functional connectivity to several target networks has been noted across amygdala subregions in a sample of children compared with adults (Qin et al., 2012), but the age-related changes in functional connectivity specific to each subregion and shared across subregions remain unknown. We characterized both the connectivity patterns differentiating each subregion in age-controlled and age-dependent analyses and assessed how these patterns converged across development to comprehensively examine the construction of amygdala networks from early childhood through adulthood.

Materials and methods

Participants

Fifty-eight children, adolescents, and adults ages 4 to 23 years (mean age (S.D.) = 13.4 (4.8); 29 females, 29 males) contributed usable resting-state MRI data for this study (for participant age distribution, see Fig. 1). Handedness assessments using the Physical and Neurological Examination for Subtle Signs (PANESS) were available for 55 participants, such that 51 participants were right-handed, 3 were left-handed, and 1 reported using both hands for daily tasks (neither the left-handed nor the ambidextrous participants were outliers in any analysis and so were included in the sample). Participants identified their ethnicity as European American (48.3%), Asian American (27.6%), African American (27.6%), American Indian (5.2%), and other (3.4%). Nineteen percent (19.0%) of participants identified as Hispanic/Latino. All participants were physically and psychiatrically healthy as confirmed by a telephone screening during recruitment. Cognitive ability was assessed using the Wechsler Abbreviated Scale of Intelligence for participants ages 6–17 years old, and the average full-scale intelligence quotient of this sample was within the average range (mean (S.D.) = 112.8 (17.2)). Data on household income were obtained from the families of child and adolescent participants, with a mean income range of $70,000–85,000. Adults in this study were matriculated undergraduate students. This study was approved by the Institutional Review Boards of the University of California, Los Angeles and the state of California. All participants provided informed consent or assent (in the case of minors) for this study.

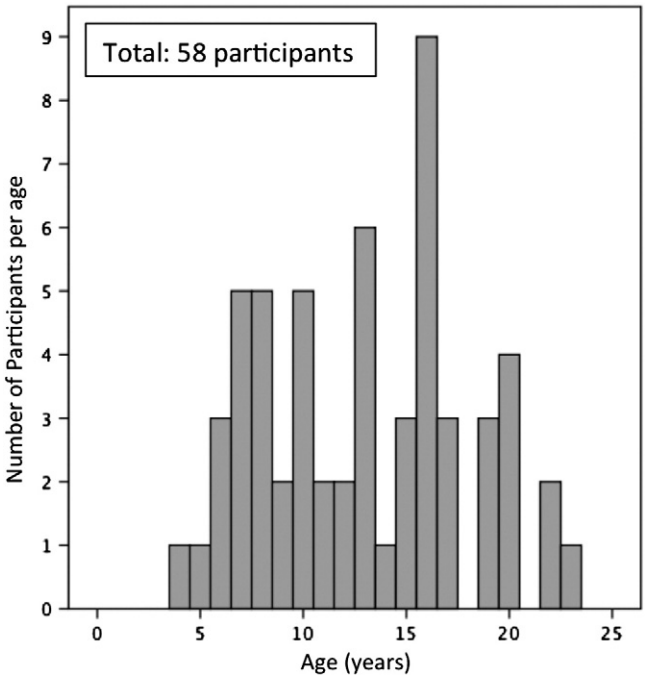

Fig. 1. Participants' age distribution.

Data acquisition

All participants were given the opportunity to acclimate to an MRI scanner environment with an MRI replica prior to the scanning session. To further avoid capturing any patterns of functional connectivity attributable to differences in initial MRI acclimation between the younger and older participants, all participants completed the resting-state scan at the end of a forty-five minute-long session that included fMRI tasks. To preclude potential carry-over effects from the fMRI tasks, the resting-state scan was directly preceded by a buffer of approximately 15 min of anatomical scans during which participants passively viewed a film. Participants were then instructed to lie still with their eyes closed (but not sleep), but were also presented with a black screen that had a white fixation cross at the center, which they viewed through video goggles (Resonance Technology, Inc., model: VisuaStim Digital, software version 8). Participant alertness was assessed through direct observation at the end of the scan as well as self-report of sleepiness. Notably, only one older participant's data were discarded due to sleep during the resting-state scan. In accordance with recent recommendations for optimal resting-state parameters, the duration of the scan was 6 min (Van Dijk et al., 2010). To comfortably stabilize participants' heads and reduce motion during the scan, cloth pads were layered underneath an air vacuum pillow (Siemens Comfort Pack) that was molded around their heads.

All participants were scanned with a Siemens Trio 3.0-Tesla MRI scanner using a standard radiofrequency head coil. We collected 180 T2*-weighted echoplanar images (33 slices, slice thickness 4 mm, skip 0 mm, field of view [FOV] 220 mm, matrix 64 × 64, TR = 2000 ms, TE = 30 ms, flip angle = 75°) at an oblique angle of approximately 20° to 30° to minimize signal drop-out. A whole brain, high resolution, T1-weighted anatomical scan (MP-RAGE; 192 × 192 inplane resolution, 256 mm FOV; 192 mm × 1 mm sagittal slices) was acquired for each subject for registration and localization of functional data to Talairach space (Talairach and Tournoux, 1988).

Data pre-processing

Motion corrections

All included data were free of movement greater than 2.5 mm or degrees in any direction (mean length of retained data = 5.73 min). Given this motion restriction, two participants could only contribute between 3.5 and 4 min of usable data (ages 4 and 8 years); however, because neither of these subjects were outliers in any analysis, and because resting-state correlation strengths have been shown to stabilize very rapidly (Van Dijk et al., 2010), these participants' data were included in analyses. Importantly, several recent reports have demonstrated that resting-state functional connectivity analyses are especially sensitive to motion artifacts (e.g. Hallquist et al., 2013; Power et al., 2012; Satterthwaite et al., 2012; Van Dijk et al., 2012), thus several further steps were taken in the processing stream to thoroughly address this potential confound. First, high-frequency signals have been shown to be most susceptible to motion confounds so all data were temporally bandpass-filtered with a more conservative cutoff of 0.08 Hz (compared to the 0.1 Hz cutoff often used for resting-state data) as recommended by Satterthwaite et al. (2012). At the within-subject level of analysis, 6 rigid body motion regressors (3 translational and 3 rotational), the 6 backward temporal derivatives of those regressors, and a global signal regressor that has been shown to ameliorate sub-millimeter motion confounds as well as white-matter and ventricle regressors were included (for a total of 15 nuisance regressors) in all regressions to correct for head motion artifacts (Van Dijk et al., 2010; Yan et al., 2013). Furthermore, at the between-subject level, the mean absolute displacement value was calculated for each subject as described in Van Dijk et al. (2012) and used as a covariate in the regressions to control for different levels of head motion between subjects. Control analyses were conducted at the group level with the mean absolute displacement values entered as the regressor of interest to check that significant motion-related effects did not overlap with the results from the primary analyses. Lastly, to again verify that motion effects were not confounding the present results, a control analysis was run employing the simultaneous regression method recently reported by Hallquist et al. (2013) as a robust correction for such potential motion effects. Results from this control analysis were consistent with the reported analyses with respect to both the significant regions identified and the valence of this connectivity with the amygdala.

Pre-processing stream

The functional imaging data were preprocessed and analyzed with the Analysis of Functional NeuroImages (AFNI) software package (Cox, 1996). For each participant's images, preprocessing included discarding the first 4 functional volumes to allow for BOLD signal stabilization, correction for slice acquisition dependent time shifts per volume, rigid body translation and rotation from each volume to the first volume to generate 6 within-subject motion regressors, and spatial smoothing with an isotropic 6-mm Gaussian kernel (FWHM) as has been standard in previous studies with amygdala subregion regions of interest (Ball et al., 2007; Qin et al., 2012; Roy et al., 2009). Volumes exhibiting motion greater than 2.5 mm or 2.5° in any direction as compared to the first functional volume were then discarded using censor files.

To allow for comparisons across individuals, timecourses were then normalized to percent signal change and transformed to the standard coordinate space of Talairach and Tournoux (1988) using parameters obtained from the transformation of each individual's high-resolution anatomical scan. Talairached transformed images had a resampled resolution of 1 mm^3 (see Appendix A for validation of young children's image registration to standard coordinate space).

A temporal band-pass filter (0.009 Hz < f < 0.08 Hz) was applied to the data to isolate the relevant signal fluctuations contributing to functional networks. Timecourses for the right ventricle, white matter, and the global signal were then extracted as nuisance covariates to account for external contamination of the remaining resting-state frequencies.

Region of interest timecourse extraction

As in Roy et al. (2009), amygdala and amygdalar subregion regions of interest (ROIs) were determined in standard space using the stereotaxic, probabilistic maps of cytoarchitectonic boundaries generated by Amunts et al. (2005) that are available in FSL's Juelich histological atlas. Maps exist for the amygdala's laterobasal (LB) subregion, centromedial (CM) subregion, and the superficial (SF) subregions for each hemisphere. Only voxels with at least a 50% probability of belonging in one of these subregions were included in an ROI, and each voxel was assigned to only one subregion. Subregion maps for the two hemispheres were combined to create bilateral ROIs for the LB, CM and SF subregions. A bilateral amygdala ROI was created by combining the bilateral LB, CM, and SF maps (see Fig. 2 inset). Average timecourses were then calculated for the bilateral amygdala and the bilateral LB, CM, and SF subregions from the band-pass filtered data.

Primary statistical analysis

For each subject, a separate regression was performed for each amygdala ROI seed region (bilateral whole amygdala, LB, CM or SF subregion). Because timecourse data violates the GLM assumption of independent residuals, AFNI's 3dREMLfit program was used to fit generalized Least Squares ARMA (1,1) regression models that correct for (prewhiten) temporal autocorrelation. Each regression model included the ROI timecourse, 12 motion regressors (6 motion files and their 6 backwards temporal derivatives), and the 3 ventricle, whitematter, and global signal nuisance regressors (for a total of 16 regressors). These regressions generated subject-level maps of the correlations between the ROI average timecourse and every other voxel's timecourse.

Group-level analysis

Age-controlled analysis

To determine significant correlations between each of the four amygdala ROIs and all other brain voxels controlling for age, we conducted a group-level mixed-effects analysis of covariance (ANCOVA) with AFNI's 3dttest++ program to identify correlations that were significantly different from zero. To control for different motion levels across subjects, each subject's mean absolute displacement value was calculated and entered along with subject age as mean-centered covariates into the group-level ANCOVA. To control the type I error rate given the multiple comparisons in each ANCOVA, whole-brain cluster-based corrections were performed using thresholds generated from Monte Carlo simulations in AFNI's 3dClustSim program (uncorrected p-value .025, corrected alpha rate of .01 for primary analyses with cluster size minimum of 3073 mm^3. Although these analyses could potentially bias results towards large clusters, secondary analyses with uncorrected p-values at .005 and cluster size minimum of 955 mm^3 revealed highly consistent results (not reported)).

Age-dependent analysis

A mixed-effects group-level linear regression using AFNI's 3dRegAna program was then conducted with these individual subject maps for each of the four amygdala ROIs to assess how correlations between the amygdala ROI and all other brain voxels change continuously with age. Pubertal stage as measured by the Peterson Pubertal Development Scale (Petersen et al., 1988) was unfortunately only collected for a subset of the participants (only those over 10 years old) but was not a significant covariate for this subsample. Sex was also evaluated as a potential covariate but no significant effects or interactions with age were identified for the regions that showed significant age-dependent change in connectivity in these analyses. Each subject's motion level (i.e. subject mean absolute displacement value) was entered into the regression as a covariate and whole-brain cluster-based corrections were performed as above.

Post-hoc piecewise non-linear least squares regressions were conducted using the "nl" procedure in STATA (version 12.1) for the regions

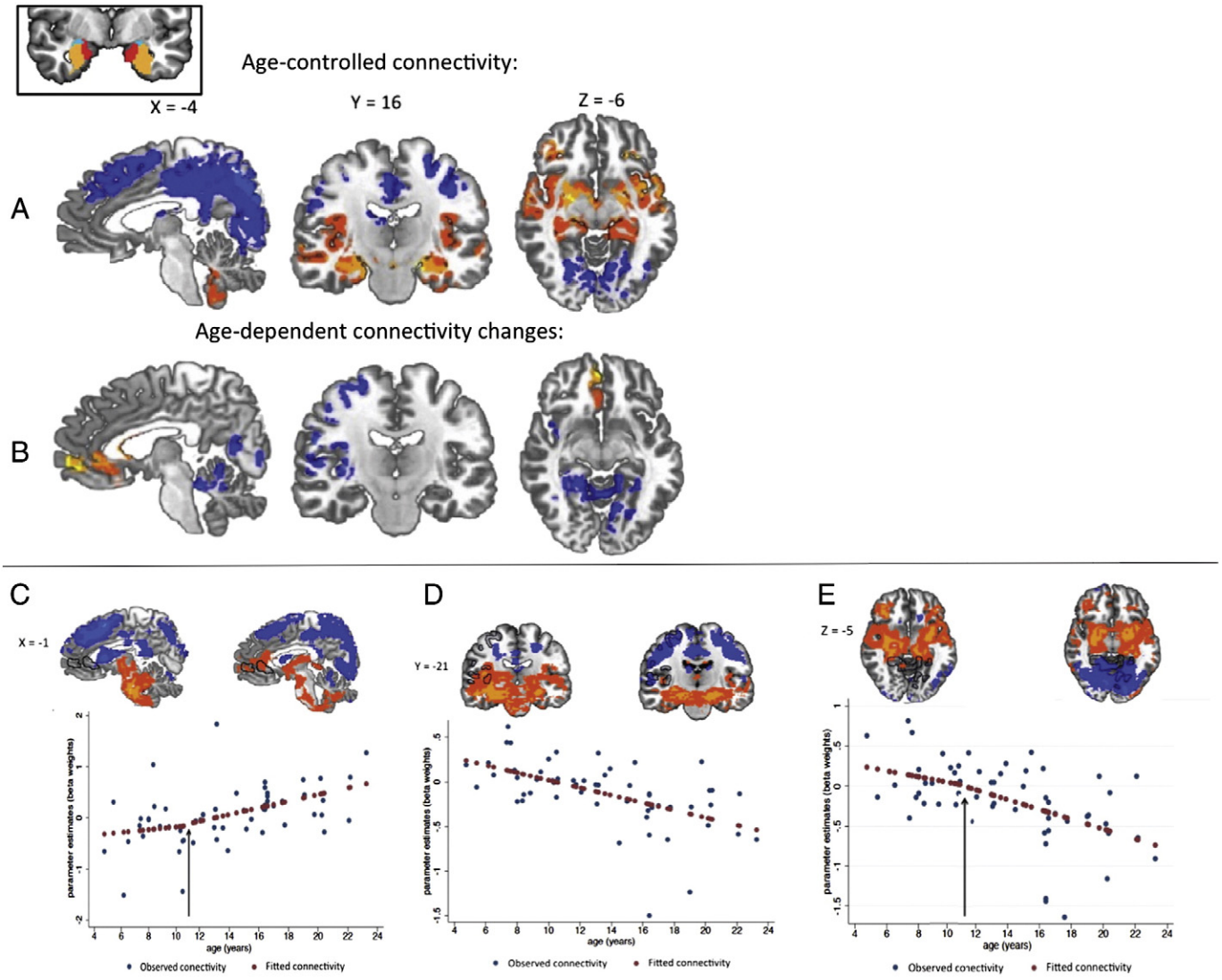

Fig. 2. Functional connectivity of the bilateral amygdala. Left corner inset: Bilateral anatomical amygdala seed region of interest comprised of the basolateral subregion (orange regions), centromedial subregion (turquoise regions) and superficial subregion (red regions) as used by Roy et al. (2009). A: Age-controlled functional connectivity, $p < .05$ whole brain corrected. Significant positive connectivity with the amygdala is shown in warm colors. Significant negative coupling with the amygdala is shown in cool colors. B: Age-dependent functional connectivity, $p < .01$ whole brain corrected. Significant changes in amygdala coupling with age were observed for a medial prefrontal cortex region (left panel), a right insula/temporal/parietal functional region (middle panel), and a cerebellar/occipital/parahippocampal functional region (right panel). C, D, E: Parameter estimates (beta weights) for functional regions with significant age-related changes in amygdala connectivity. Observed parameter estimates for the sample are indicated by blue markers. Fitted parameter estimates from post-hoc piecewise regressions are indicated by red markers. Regions of interest identified in the age-dependent analysis are traced in black on images of coupling at youngest (ages 4 to 9, $n = 16$) and oldest (ages 16 to 23, $n = 16$) ages for illustrative purposes only. C: connectivity with the medial prefrontal cortex region changes from zero to positive coupling. The black arrow marks the age 10.5 identified in post-hoc piecewise regression as the age when this positive connectivity first appears. D: connectivity with the insula/temporal/parietal region across age changes from positive to negative coupling. E: Connectivity with the cerebellar/occipital/parahippocampal region changes from zero to negative coupling. The black arrow marks the age 11.25 years that post-hoc piecewise regression identified as the age when this negative connectivity first appears.

of age-dependent changes in connectivity that did not show any significant connectivity in childhood to identify the age at which connectivity first began to appear. That is, we modeled and assessed the potential presence of a cut-point in age, measured continuously in months, after which the slope of the connectivity was different from the slope before the cut-point. The cut-points (inflection points) were thus empirically derived. These non-linear regressions were not used to evaluate the overall significance of any period of connectivity change as that had already been assessed by the age-dependent analysis.

Subregion analyses

Two different analyses were performed for the amygdala subregions to distinguish age-related changes in connectivity unique to each subregion that provided overlapping as well as unique information about these three subregions.

Orthogonal (masking approach). First, masking analyses between the amygdala subregion ROI group-level cluster-corrected maps were then performed as in the corresponding report with adults (Roy et al., 2009) to isolate brain regions with correlation changes unique to each subregion (i.e. the areas where only that single subregion shows age-related changes in correlation): CM orthogonal to the LB and SF, LB orthogonal to the CM and SF, and SF orthogonal to the CM and LB. For example, to attain the region-unique LB connectivity changes in this analysis, the complete LB age-dependent connectivity map had all regions where either the SF or CM showed significant connectivity masked out, leaving only regions with age-dependent connectivity changes for the LB. Although this analysis indirectly tests age-related changes in connectivity between subregions (e.g. voxels are first statistically tested against 0 for each subregion after which these maps are then compared across subregions), this analysis allowed for subregions' age-related changes to be compared with the mature subregion

segregation patterns previously reported using this same approach (Roy et al., 2009).

Conjunction (masking approach). The single subregion regression cluster-corrected ROI maps from the group-level were also subjected to a conjunction analysis to determine regions where correlation changes converged for multiple subregions. The group-level cluster-corrected subregion maps were overlaid such that voxels with significant correlation change for two or three subregions were preserved in the analysis. This approach uniquely identified areas where multiple subregions showed the same age-related changes in connectivity.

Orthogonal (contrast approach). Direct tests of age-related changes in connectivity between subregions were also performed using contrast regressions to identify areas where one subregion's change in connectivity was significantly different from that of the other two subregions (e.g. LB age-related changes > CM + SF age-related changes). For these analyses, single-subject regressions were run with all three contrasts of interest (an LB contrast, CM contrast, and SF contrast) as well as the typical 15 nuisance regressors previously described and then submitted to group-level regression to identify age-related changes for each contrast separately. These analyses also confirmed the lack of differences between amygdala subregion connectivity changes across age for the mPFC region of interest, the single region that showed uniform convergence in the conjunction analyses.

Secondary statistical analyses

A global regressor was included in the primary analyses in this study for several reasons. Although it has been clearly shown that global signal regression can induce spurious negative correlations between regions' signals (Murphy et al., 2009; Saad et al., 2012; Weissenbacher et al., 2009), this regression provides several important advantages. Foremost, including a global signal facilitates comparison and continuity with the results of the recent adult resting-state amygdala connectivity analyses performed by Roy et al. (2009), which included a global signal regressor. In addition, including the global signal has the advantage of modeling physiological noise that requires removal from the data, but whose sources (heart rate and respiration) were not possible to measure directly in this study or parse out with programs like PESTICA (designed to model adult physiological noise) (Chang and Glover, 2009; Fox et al., 2009). This signal has also been shown to reduce the effects of insidious sub-millimeter motion confounds (Van Dijk et al., 2010; Yan et al., 2013). As both the physiological noise and sub-millimeter motion levels may differ between children and young adults, including this global signal provided a way to minimize the age-related differences in these confounds. Because the use of global signal regression in resting-state analyses is currently a matter of debate for the field (e.g. Chen et al., 2012; He and Liu, 2012; Saad et al., 2012), parallel regression analyses were conducted without global signal regressors to corroborate the results from the primary analyses.

In these secondary analyses, the average correlation between the amygdala ROI and every other brain voxel was calculated (as in Hampson et al., 2010) for each subject and entered as an additional covariate in the group-level regression model to account for whole-brain signal correlation without inducing spurious negative correlations. Notably, we did not find significant differences between the youngest and oldest participants' average whole-brain correlations ($p = 0.15$), suggesting that a "global" shift with age in correlation strength between the amygdala and the rest of the brain is not responsible for the age-related effects observed in the primary analyses. Importantly, in these secondary analyses without global signal, physiological differences are no longer accounted for in any capacity and the resulting group level results display evidence of these artifacts, hindering whole-brain interpretation of the data and appearing in the insula/STS/G region of interest identified in the primary analyses. Still, results from these secondary analyses for the regions of interest identified in the global-signal regression analyses were consistent with the primary analyses that included global signal regression, especially for the mPFC and posterior cerebellum regions free of physiological artifact, where both the positive and negative correlations and their respective age-related shifts were replicated.

Results

Whole bilateral amygdala

Age-controlled functional coupling with the amygdala

We used ANCOVA to identify functional coupling with the amygdala (coupling parameters that were significantly different from zero), controlling for age and subject motion effects (whole-brain corrected $p < 0.05$). This analysis revealed that there was functional connectivity between the amygdala and the ventral/limbic and dorsal/posterior regions that was constant across this age-range. Specifically, the amygdala showed positive coupling with ventral and limbic regions including the bilateral insula, striatum, thalamus, and parahippocampal gyrus that did not change with age (Fig. 2A, Table 1). Conversely, the amygdala showed negative coupling with dorsal and posterior regions including the bilateral middle frontal gyrus, superior frontal gyrus, dorsal parietal lobes, and occipital lobes that did not change with age (Fig. 2A, Table 1). This analysis controlling for age effects replicated the amygdala coupling patterns previously identified in adults except for coupling with three regions: the medial prefrontal cortex (mPFC), the superior temporal sulcus/insula, and the region including the posterior cingulate and parahippocampal gyrus (Roy et al., 2009).

Age-dependent changes in functional coupling with the amygdala

In order to examine age-dependent changes in functional coupling with the amygdala, we used regression analysis with age as an independent variable of interest, controlling for subject motion (whole-brain corrected to a stricter threshold of $p < 0.01$). Importantly, although our primary analysis presented here included a global signal regressor at the subject level (for reasons detailed in the Materials and methods

Table 1
Age-controlled functional connectivity with the whole bilateral amygdala.

Structure	BA	Voxels (mm^3)	Peak coordinates (x, y, z)
Positive connectivity			
Uncus-L,R		85,123	−22, −11, −15
Amygdala-L,R			
Hippocampus-L,R			
Parahippocampal gyrus-L,R	27, 34		
Fusiform gyrus-L,R	36		
Cerebellum tonsil-L,R			
Thalamus-L,R			
Globus pallidus-L,R			
Putamen-L,R			
Ventral superior temporal gyrus-L,R	38		
Insula-L,R	13		
Claustrum-L,R			
Inferior frontal gyrus-L,R	47		
Negative connectivity			
Paracentral gyrus-L,R	5	88,684	−1, −71, 40
Inferior parietal lobe-L,R	40		
Precuneus-L,R	19, 7		
Cuneus-L,R	17		
Lingual gyrus-L,R	18		
Middle occipital gyrus-L,R	19		
Inferior occipital gyrus-L			
Cingulate gyrus-L,R	31, 23, 30		
Middle frontal gyrus-L,R	8, 9	52,078	−23, 55, 12
Superior frontal gyrus-L,R	6, 8, 9		
Medial frontal gyrus	6, 8		
Precentral gyrus-L,R	4, 6		
Cingulate gyrus-L,R	32		
Caudate-R		3282	1, −18, 18
Thalamus-L, R			

Table 2
Age-dependent changes in functional connectivity (FC) with the whole bilateral amygdala.

Structure	BA	Voxels (mm^3)	Peak coordinates (x, y, z)	Direction of change with increasing age	Child FC	Adult FC
Medial prefrontal cortex region		3819	4, 51, −4	↑	No	+
Medial frontal gyrus	10, 32					
Ventral anterior cingulate cortex	32, 24					
Insula/temporal/parietal region		21,047	52, −38, 11	↓	+	−
Posterior insula-R	13					
Superior temporal gyrus/sulcus-R	22, 41					
Inferior parietal lobe-R	40					
Claustrum/anterior insula-R	13					
Posterior cingulate/parahippocampal region		18,045	20, −38, −10	↓	No	−
Posterior cingulate-R	30, 31					
Parahippocampal gyrus-L,R	35, 36					
Cuneus-L,R	17, 18					
Culmen-L,R						

section above), we also conducted a parallel regression analysis without this subject-level global signal regressor and obtained consistent results. Therefore, we are confident that functional regions and their age-related changes in coupling with the amygdala were not observed due to the inclusion of the global signal regressor. This analysis revealed three functional regions that showed linear age-dependent changes in connectivity. Notably, these were the regions absent from the age-*controlled* findings. These regions included a mPFC region, and two broadly defined functional regions: one region composed of right insula and temporal–parietal regions, and the other composed of posterior regions (largely the posterior cingulate and parahippocampal gyrus) (Fig. 2B, Table 2). These three regions differed in the valence of functional coupling at both younger and older ages. We discuss each of these regions in turn below.

Age-dependent mPFC–amygdala coupling. The amygdala coupling with the mPFC (comprised of medial frontal gyrus and ventral anterior cingulate cortex (ACC)) became increasingly positive with increasing age (Fig. 2B, Table 2). A post-hoc piecewise regression analysis controlling for subject motion revealed that positive coupling between these regions first appeared at age 10.5 years (cutpoint at 10.5 years, $p = .036$), after which this positive coupling increased with age (Fig. 2C). That is, younger age was associated with no initial coupling between the amygdala and the mPFC, while older age was associated with strong positive coupling.

Age-dependent insula/temporal/parietal–amygdala coupling. The amygdala coupling with the region including the right insula, right superior temporal gyrus/sulcus (STG/S), and the right inferior parietal lobe became increasingly negative with increasing age (Fig. 2B, Table 2). Post-hoc t-tests, controlling for subject motion, confirmed that children exhibited significantly positive coupling (ages 4 to 9, $n = 13$, $p < .05$, corrected) while adults had significantly negative coupling between this functional region and the amygdala (ages 17 to 23, $n = 13$, $p < .05$, corrected). That is, younger age was associated with significant positive coupling between these regions, whereas older age showed significant negative coupling between these regions (Fig. 2D).

Age-dependent posterior cingulate/parahippocampal–amygdala coupling. The amygdala coupling with a bilateral functional cluster of regions including the posterior cingulate, parahippocampal gyrus, and cerebellum became increasingly negative with increasing age (Fig. 2B, Table 2). Post-hoc piecewise regression controlling for subject motion confirmed that children had no significant coupling between the amygdala and these regions, and revealed that negative coupling first appeared at age 11.25 years (cutpoint at 11.25 years, $p = .01$), after which this negative coupling significantly increased with age (Fig. 2E). That is, younger age was associated with no initial coupling between the amygdala and this region cluster, while older age was associated with negative coupling between these regions.

Amygdala subregions

Laterobasal subregion

Age-controlled functional coupling with the laterobasal subregion. The ANCOVA controlling for age and subject motion effects (whole-brain corrected $p < 0.05$ for this and all other subregions) revealed that functional connectivity between the laterobasal (LB) amygdala subregion and primarily posterior and dorsal regions was constant across this age-range (Fig. 3A, Table 3). Although the LB showed positive connectivity with ventral regions including bilateral amygdala, bilateral parahippocampal gyrus, and bilateral fusiform gyrus, the LB was predominantly negatively coupled with regions after controlling for age, including bilateral dorsal cingulate gyrus, bilateral occipital lobes, and the left parietal lobe (Fig. 3A, Table 3).

Age-dependent changes in functional coupling with the laterobasal subregion. Age-dependent changes in functional coupling with the LB subregion (whole-brain corrected $p < 0.05$ for this and all other subregions) were observed primarily in frontal, dorsal, and posterior regions (Table 4). The LB coupling with a prefrontal cortex region comprised of medial frontal gyrus, Brodmann Area 10, and anterior cingulate cortex became increasingly positive with increasing age (Fig. 3B). Conversely, the LB coupling with exclusively dorsal and posterior regions, especially in the parietal and occipital lobes, became increasingly negative with increasing age (Fig. 3B).

Fig. 3. Functional connectivity of amygdala subregions. For each age-controlled panel (A, C, E), significant positive connectivity is shown in warm colors and significant negative coupling is shown in cool colors, $p < 0.05$ whole brain corrected. For each age-dependent panel (B, D, F), coupling that becomes increasingly positive with increasing age is shown in warm colors, and coupling that becomes increasingly negative with increasing age is shown in cool colors, $p < 0.05$ whole brain corrected. A: Age-controlled functional connectivity with the laterobasal (LB) subregion, B: age-dependent functional connectivity with the LB subregion. Coupling with a medial prefrontal cortex region became increasingly positive with increasing age, and coupling with dorsal and posterior regions became increasingly negative with increasing age. C: age-controlled functional connectivity with the centromedial (CM) subregion, D: age-dependent functional connectivity with the CM subregion. Coupling with a medial prefrontal region and a left dorso-lateral prefrontal region became increasingly positive with increasing age. Coupling with ventral regions became decreasingly positive with increasing age such that positive connectivity became weaker, but remained significantly positive with older age. E: Age-controlled functional connectivity with the superficial (SF) subregion, F: age-dependent functional connectivity with the SF subregion. Coupling with a medial prefrontal cortex region became increasingly positive with increasing age. Coupling with primarily ventral and limbic regions became increasingly negative with increasing age.

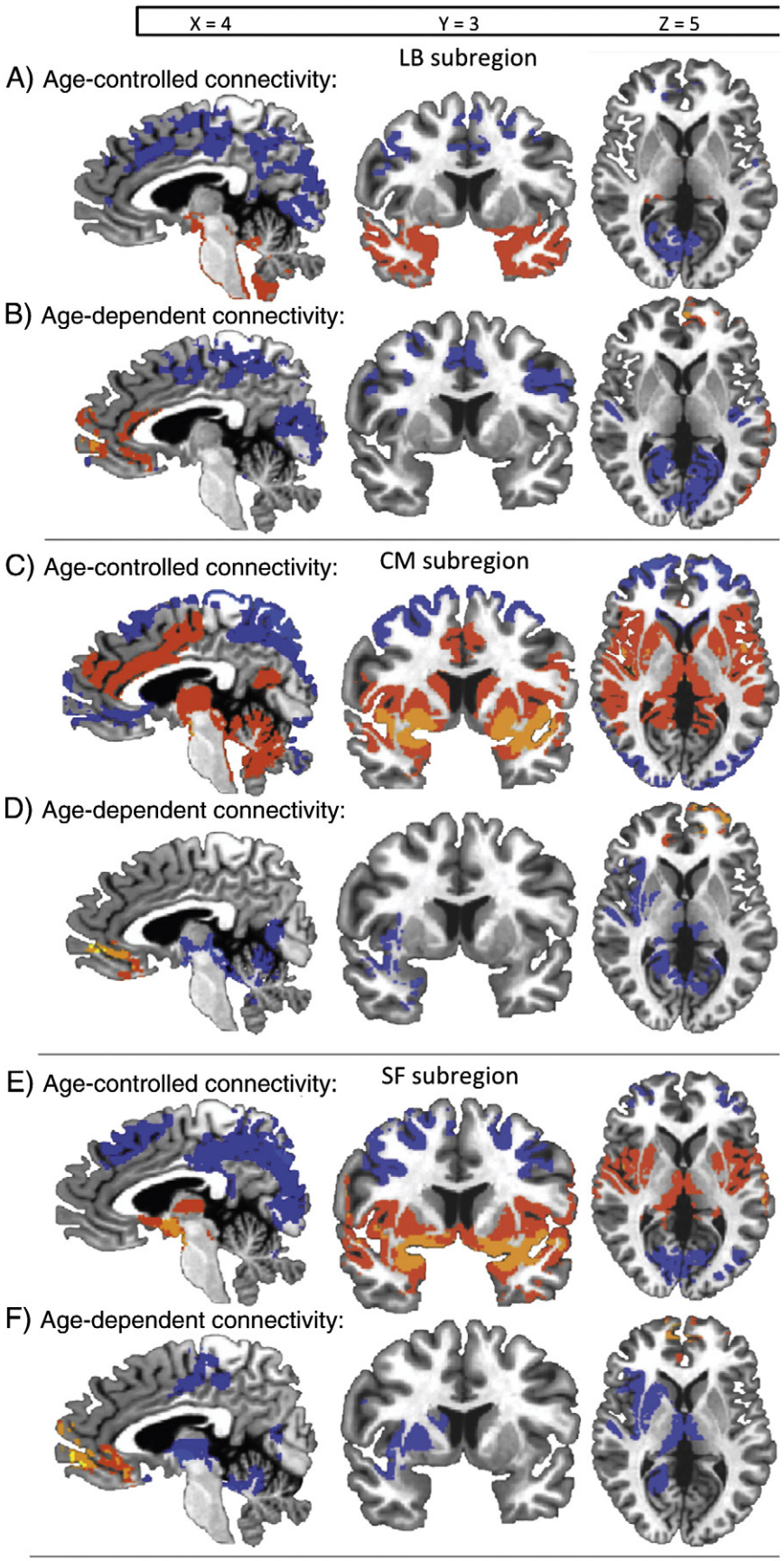
X = 4
Y = 3
Z = 5
LB subregion
A) Age-controlled connectivity:
B) Age-dependent connectivity:
CM subregion
C) Age-controlled connectivity:
D) Age-dependent connectivity:
SF subregion
E) Age-controlled connectivity:
F) Age-dependent connectivity:

Table 3
Age-controlled functional connectivity with the bilateral laterobasal subregion.

Structure	BA	Voxels (mm^3)	Peak coordinates (x, y, z)
Positive connectivity			
Uncus-L,R		73,149	−55, −1, −4
Amygdala-L,R			
Hippocampus-L,R			
Parahippocampal gyrus-L,R	34, 35		
Cerebellum-L,R			
Culmen-L,R			
Fusiform gyrus-L,R	36		
Ventral superior temporal gyrus/sulcus-L,R	38		
	21		
Ventral middle temporal gyrus/sulcus-L,R	47		
Ventral inferior frontal gyrus-L,R			
Negative connectivity			
Cerebellum-L,R		34,878	−1, −71, 36
Fusiform gyrus-L,R			
Occipital lobe-L,R			
Lingual	18, 19		
Cuneus	17, 18, 19		
Precuneus-L,R	7		
Inferior parietal lobe-L	40		
Transverse temporal gyrus/sulcus-L	41, 32, 24		
Dorsal cingulate gyrus-L,R	2		
Postcentral gyrus-L	6		
Precentral gyrus-L	40		
Supramarginal gyrus-L	13		
Insula-L			
Paracentral lobule-L,R		14,395	−5, 50, 14
Cingulate gyrus-L,R	31, 24		
Dorsal medial anterior cingulate cortex-L,R	32, 24		
Medial frontal gyrus-L,R	9		
Dorsal medial frontal gyrus-R	9, 8, 6	7336	52, 19, 26
Superior frontal gyrus-R	9, 8		
Dorsal middle frontal gyrus-R	9, 6		

Orthogonal analyses. Two orthogonal analyses were performed to address age-related changes in amygdala subregion connectivity. Using the orthogonal (masking approach) analyses (as in Roy et al., 2009), age-dependent changes in functional coupling unique to the LB (orthogonal to the coupling of the other two subregions) were determined by simultaneously comparing the significant coupling patterns for all three regions (whole-brain corrected $p < 0.05$ for all subregions) and identifying regions showing coupling changes with only the LB subregion. Age-dependent coupling changes unique to the LB occurred in two functional regions: a dorsal region and a posterior region. The dorsal region included bilateral precuneus, pre and postcentral gyri, dorsal cingulate gyrus, left inferior parietal lobe and left insula. The posterior region included bilateral cerebellum, posterior cingulate gyri, and occipital lobes (Table 4 starred entries). For both the dorsal and posterior functional regions, younger age was associated with no significant coupling between these regions and the LB, whereas older age was associated with significant negative coupling between these regions and the LB (Table 4 starred entries). Orthogonal (contrast approach) analyses revealed highly consistent results with this orthogonal masking approach as shown in Fig. 5 and Table 9.

Centromedial subregion

Age-controlled functional coupling with the centromedial subregion. The ANCOVA controlling for age and subject motion effects revealed that functional connectivity between the centromedial (CM) amygdala subregion and posterior, ventral, and anterior dorsal regions was constant across this age-range (Fig. 3C, Table 5). While the CM had negative coupling with a posterior occipital/parietal region, the CM showed primarily positive connectivity with ventral, sensory/motor regions such as the amygdala, thalamus, and cerebellum as well as anterior dorsal regions including the anterior cingulate cortex and medial frontal gyrus after controlling for age (Fig. 3C, Table 5).

Age-dependent changes in functional coupling with the centromedial subregion. Age-dependent changes in functional coupling with the CM amygdala subregion were observed mostly in anterior and ventral regions (Table 6). The CM coupling with medial and left dorso-lateral frontal gyrus regions became increasingly positive with increasing age, while coupling with ventral sensory/motor regions became decreasingly positive with increasing age (although this coupling remained significantly positive in adults) (Fig. 3D).

Orthogonal analyses. Using the orthogonal (masking approach) analyses (as in Roy et al., 2009), age-dependent changes in functional coupling

Table 4
Age-dependent changes in functional connectivity (FC) with the bilateral laterobasal subregion.

Structure	BA	Voxels (mm^3)	Peak coordinates (x, y, z)	Direction of change with increasing age	Child FC	Adult FC
*Cerebellum-L,R		32,489	4, −73, 38	↓	No	−
Parahippocampal gyrus-L,R						
*Posterior cingulate gyrus-L,R	30,31,23					
Occipital lobe-L,R						
(* L) Lingual gyrus	18					
*Cuneus	17, 18					
*Precuneus-L,R	7					
Precuneus-L,R	7	41,285	−48, −20, 50	↓	No	−
*Inferior parietal lobe-L	40					
Superior temporal gyrus/sulcus-L	22					
*Insula-L	13					
(* L) Postcentral gyrus-L,R	3					
*Paracentral lobule-L,R	5					
*Precentral gyrus-L,R	4, 6					
*Dorsal cingulate gyrus-L,R	24, 31					
Medial frontal gyrus-L,R	6					
*Middle frontal gyrus-R	6, 8					
*Inferior parietal lobe-R	40	13,721	42, −38, 47	↓	No	−
*Superior parietal lobe-R						
*Precuneus-R	7					
*Post-central gyrus-R	3					
Medial frontal gyrus-L	10, 32	7457	0, 52, 36	↑	No	+
Anterior cingulate cortex-L,R	24					

* Indicates regions where laterobasal connectivity is orthogonal to superficial and centromedial subregion connectivity (masking approach).

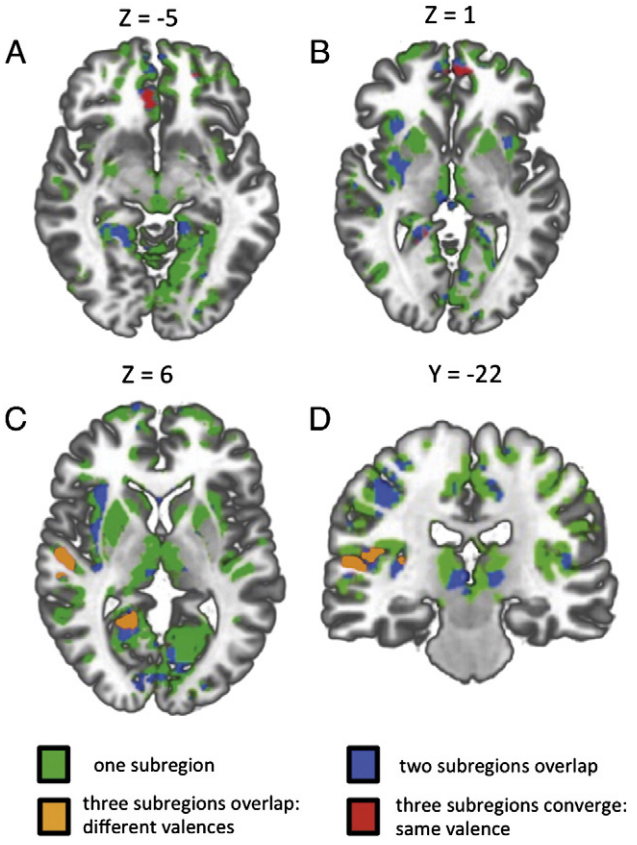

Fig. 4. Conjunction (masking approach) analysis regions of convergence for all three subregions. Functional regions that demonstrated the same nature of age-dependent functional connectivity changes across all three subregions are indicated in red. Functional regions that demonstrated different age-dependent functional connectivity changes across all three subregions are indicated in orange. Regions with age-dependent connectivity changes with two of the three subregions are indicated in blue. Regions with age-dependent connectivity changes with any one of the subregions are indicated in green. All functional regions are significant at $p < .05$ whole brain corrected. A: Anterior cingulate cortex region of convergence. B: medial frontal gyrus region of convergence. C: Right superior temporal gyrus/sulcus and right posterior cingulate/parahippocampal regions of convergence. D: Right insula region of convergence.

unique to the CM (when simultaneously compared with patterns for the laterobasal and superficial subregions) occurred in two functional regions: a left dorsolateral PFC region and a ventral sensory/motor region.

Specifically, a change in CM coupling with the left dorsolateral PFC was observed where younger age was associated with no significant coupling, and older age was associated with significant positive coupling (Table 6 starred entries). Conversely, a change in CM coupling with the ventral sensory/motor region that included bilateral parahippocampal gyrus, red nucleus, and right amygdala and insula was found where younger age was associated with strong positive connectivity, while older age was associated with weaker positive connectivity (Table 6 starred entries). Orthogonal (contrast approach) analyses revealed highly consistent results with this orthogonal masking approach as shown in Fig. 5 and Table 10.

Superficial subregion

Age-controlled functional coupling with the superficial subregion. The ANCOVA controlling for age and subject motion effects revealed that functional connectivity between the superficial (SF) amygdala subregion and extensive ventral, dorsal, and posterior regions was constant across this age-range (Fig. 3E, Table 7). The SF showed positive connectivity with ventral regions including the amygdala, thalamus, lentiform nucleus, and caudate, controlling for age. In contrast, the SF showed negative coupling with a dorsal region including bilateral dorsal cingulate gyri, medial frontal gyri, superior frontal gyri, and precentral gyri (Fig. 3E, Table 7). Negative coupling was also observed between the SF and a posterior region including the cerebellum and the occipital lobes (Fig. 3E, Table 7).

Age-dependent changes in functional coupling with the superficial subregion. Age-dependent changes in functional coupling with the SF amygdala subregion were observed mostly in anterior and right-lateralized ventral regions (Fig. 3F, Table 8). The SF coupling with a medial PFC and ventral anterior cingulate cortex region became increasingly positive with increasing age (Fig. 3F). The SF coupling with ventral regions primarily in the right hemisphere, including the right lentiform nucleus, insula, and caudate became decreasingly positive with increasing age, and SF coupling with the cerebellum and right-lateralized parahippocampal gyrus and posterior cingulate gyrus became increasingly negative with increasing age (Fig. 3F, Table 8).

Orthogonal analyses. Using the orthogonal (masking approach) analyses (as in Roy et al., 2009), age-dependent changes in functional coupling unique to the SF (when simultaneously compared with patterns for the laterobasal and centromedial subregions) occurred in a ventral limbic region, including the bilateral thalamus, right globus pallidus, insula, caudate, and STG/S, such that younger age was associated with positive coupling with the SF, while older age was associated with no significant coupling with the SF (Table 8 starred entries). Orthogonal (contrast approach) analyses revealed highly consistent results with this orthogonal masking approach as shown in Fig. 5 and Table 11.

Comparison of conjunction and orthogonal analyses across subregions

The patterns of age-dependent changes in functional coupling for the LB, CM, and SF subregions were also compared simultaneously in contrast regressions and a conjunction analysis to identify regions whose coupling significantly changed across age with multiple amygdala subregions. Changes in coupling across all three subregions spatially overlapped for a mPFC region including medial frontal gyrus and ventral ACC, the right insula, the right STG/S, the right posterior cingulate, and the right parahippocampal gyrus (Fig. 4).

Notably, the only region that showed uniform (that is, converged with the same valence and spatial loci) age-related changes in coupling with all three subregions was the mPFC region, such that younger age was associated with no significant coupling while older age was associated with positive coupling for all three subregions (Figs. 4 panels A, B). This convergence was confirmed with all three subregion analyses (orthogonal (masking approach), orthogonal (contrast approach), and conjunction analysis). For all other regions of convergence opposite changes in coupling were observed across the three subregions. For example, in both the right insula and STS/G regions of convergence, older age was associated with positive coupling with the CM and SB subregions while older age was associated with negative coupling with the LB subregion (Figs. 4 panels C, D and 5). Moreover, in the right posterior cingulate and right parahippocampal gyrus regions of convergence, older age was associated with positive coupling with the SF subregion, negative coupling with the LB subregion, and no coupling with the CM subregion (Figs. 4 panel C and 5).

Discussion

We used resting-state fMRI across an extensive developmental period from age 4 to 23 years old in a cross-sectional design to map the whole-brain patterns of functional coupling with the bilateral amygdala that were stable across this period as well as to characterize the trajectories and patterns of age-related changes in coupling. Resting-state fMRI has been shown to index the stability and integrity of connections in functional networks, possibly reflecting the development of

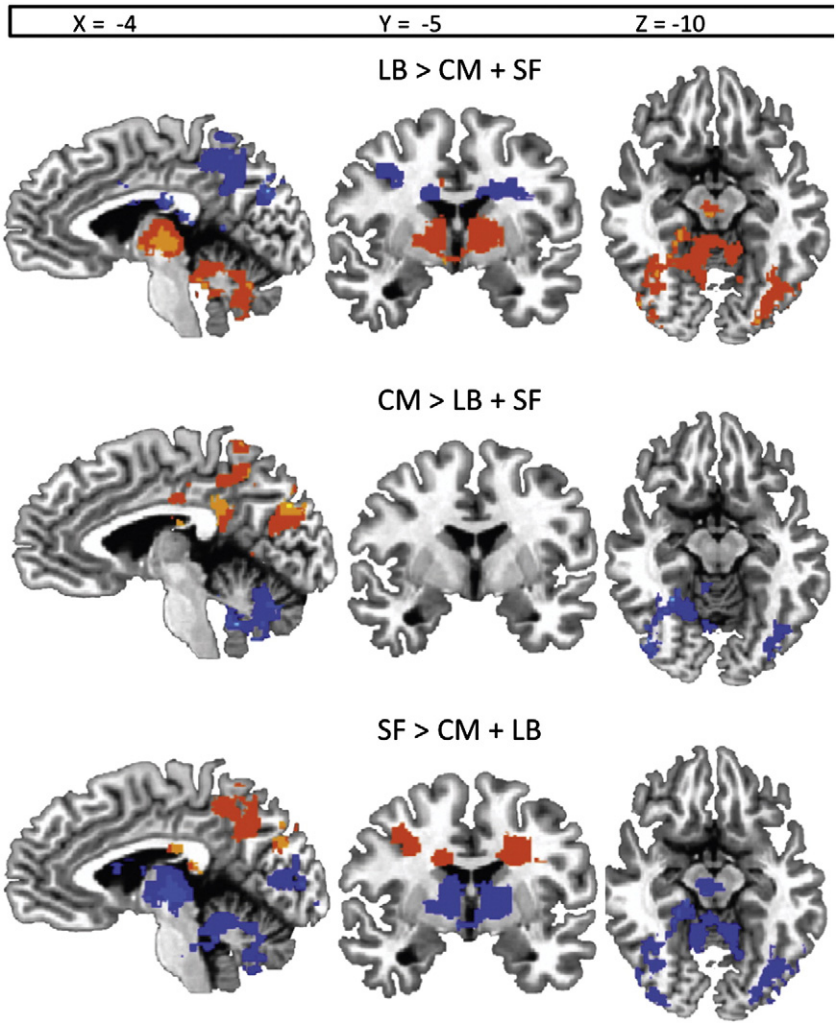

Fig. 5. Orthogonal (contrast approach) analysis regions of distinct connectivity between amygdala subregions. Functional regions where one amygdala subregion's age-related change in functional connectivity was significantly different from that of the other two subregions, as directly assessed with contrast regressions (e.g. regions where LB subregion age-related change in connectivity is significantly different from that of CM subregion and SF subregion is shown for the LB > CM + SF contrast, and likewise for CM and SF specific contrasts). Warm colors denote where that subregion had more positive age-dependent changes in connectivity than the other two subregions, and cool colors show where that subregion had more negative age-dependent changes in connectivity than the other two subregions. All functional regions are significant at $p < .05$, whole brain corrected.

synaptic connections and maintenance of synaptic homeostasis at the physiological level, and was therefore an ideal approach for assessing the trajectories of construction and stabilization of amygdala functional connections across development (Pizoli et al., 2011; Raichle, 2010; Uddin et al., 2010; Van den Heuvel and Hulshoff Pol, 2010). We found that: 1. amygdala connectivity with subcortical and limbic regions was largely stable across this developmental period, 2. amygdala functional coupling with the mPFC, insula/STS, and a posterior region including posterior cingulate and parahippocampal gyrus exhibited changes from early childhood through adulthood characterized by the appearance of both positively and negatively correlated coupling patterns, 3. the transition from childhood to adolescence around 10 and 11 years old (depending on the cortical region) marked an important point of change in the nature of amygdala–cortical functional connectivity, 4. anatomical subregions of the amygdala demonstrated changes in functional connectivity from early childhood through adulthood with unique patterns of functional network construction, and 5. age-related changes in functional connectivity for these amygdala subregions also converged on several target cortical regions, largely characterized by different connectivity valences across subregions, with the exception of universally increasing positive coupling across age with a mPFC region. Below we discuss the implications of these findings for understanding the nature of amygdala functional connectivity trajectories supporting affective and cognitive development.

Age-constant connections

We first identified functional networks whose connectivity with the amygdala was present and stable at rest in young childhood and remained constant with age. We found that subcortical and limbic regions associated with generating affective states, such as the ventral striatum and anterior insula, were positively coupled with the amygdala during this developmental period, consistent with the mature positive coupling pattern identified in adults and in animal models (Pitkänen, 2000; Roy et al., 2009). This result suggests that the functional connections of this amygdala network stabilize extremely early in human development, largely before childhood. Future studies should directly assess the early formation of this subcortical and limbic functional network during infancy and assess how these developing connections interact with the precocious structural and functional development of the amygdala that occurs during this period (Gilmore et al., 2012; Ulfig et al., 2003). Moreover, we identified patterns of negative coupling with the amygdala that remained stable across age in this sample that were largely consistent with the dorsal and posterior regions previously

Table 5
Age-controlled functional connectivity with the bilateral centromedial subregion.

Structure	BA	Voxels (mm^3)	Peak coordinates (x, y, z)
Positive connectivity			
Uncus-L,R		158,729	20, −12, 70
Amygdala-L,R			
Cerebellum-L,R			
Parahippocampal gyrus-L,R	34, 27		
Fusiform gyrus-L,R	36		
Posterior cingulate gyrus-L,R	30, 23, 29		
Thalamus-L,R			
Globus pallidus-L,R			
Putamen-L,R			
Superior temporal gyrus/sulcus-L,R	22, 41, 42		
Precentral gyrus-L,R	4, 6		
Dorsal inferior frontal gyrus-L	44		
Claustrum-L,R			
Insula-L,R	13		
Caudate-L,R			
Dorsal cingulate gyrus-L,R	24, 32, 31	14,930	2, 30, 10
Dorsal anterior cingulate cortex-L,R	24, 32		
Dorsal medial frontal gyrus-L,R	9, 6		
Negative connectivity			
Posterior cerebellum-L,R		166,224	−1, −45, 64
Occipital gyrus-L,R	17, 18, 19		
Cuneus-L,R	17, 18		
Precuneus-L,R	7		
Angular gyrus-L,R	39		
Superior parietal lobe-L,R	7		
Dorsal middle frontal gyrus-L,R	6, 8, 9, 10, 46		
Ventral anterior cingulate cortex-L,R	32, 24		

found in adults, although such negative coupling is presently difficult to interpret given the use of global signal regression for this analysis (Roy et al., 2009). In sum, our analysis of functional connectivity that was stable across age for our developmental sample replicated the amygdala coupling patterns with each region identified in the previous study with adults *except for* three significant regions discussed below that demonstrated linear age-related changes in coupling with the amygdala.

Age-dependent connectivity

We found that amygdala–cortical functional connections with three regions were characterized by age-related changes that continued through adulthood. First, an age-related increase in connectivity between the amygdala and the mPFC continued through the upper bound of our developmental sample at age 23, an extended change that supports both behavioral and fMRI-task literature indicating an extensive developmental period for these regions (e.g. Gee et al., 2013; Hare et al., 2008; McRae et al., 2012; Perlman and Pelphrey, 2011). This amygdala–mPFC circuit has been shown to be the primary neural substrate of emotion processing and regulation and has a critical role in arousal regulation with causal influence on physiological signals like skin conductance responses (e.g. Banks et al., 2007; Etkin et al., 2006, 2011; Fisher et al., 2009; Gee et al., 2013; Goldin et al., 2008; McRae et al., 2012; Hare et al., 2008; Hariri et al., 2003; Kim et al., 2011a; Linnman et al., 2012; Perlman and Pelphrey, 2011; Phan et al., 2005; Phelps et al., 2001; Zhang et al., 2013). The strong positive coupling in these adult participants is consistent with the mature pattern found in previous adult studies (Kim et al., 2011b; Qin et al., 2012; Roy et al., 2009). Secondly, we found that coupling between the amygdala and a cluster of regions including right posterior cingulate, parahippocampal gyrus, precuneus, and cerebellum became increasingly negative through adulthood (seen both with and without global signal regression), replicating negative coupling in adulthood and consistent with the trajectories of functional development of these regions that in adulthood have been associated with episodic memory, emotion, and self-related processing in concert with the amygdala (Lou et al., 2004; Luna et al., 2001; Maddock et al., 2003; Roy et al., 2009; Tottenham and Sheridan, 2009; ventral precuneus: Zhang and Li, 2012). Lastly, the amygdala demonstrated a reversal in coupling valence across age with a right-lateralized region of insula, STS/G, and inferior parietal lobe (observed more robustly in the primary global signal regression analyses), an area whose connectivity with the amygdala has been implicated broadly in emotion and face-processing paradigms, such that positive coupling in childhood switched to negative coupling by adulthood (Baseler et al., 2012; Pessoa and Adolphs, 2010; Sarkheil et al., 2012). This negative coupling was largely consistent with mature coupling patterns reported previously (Roy et al., 2009; Zhang and Li, 2013). These age-related changes in both the nature and strength of amygdala–cortical functional connectivity suggest a steady refinement of coupling patterns across childhood and adolescence.

Importantly, we identified preliminary age-related change-points in amygdala–cortical functional connectivity that occur at the transition between childhood and adolescence. Specifically, we found no significant mPFC–amygdala coupling in early childhood, and adult-like connectivity first emerged in those older than 10 years of age. Similarly, this transition from late childhood to early adolescence marked a change-point in resting functional coupling for the amygdala–posterior cortical network including posterior cingulate and parahippocampal gyrus as well. Amygdala coupling with this posterior cluster of regions was not present in childhood, but negative coupling appeared after age 11 years. Although the participants in this sample were well-distributed across the age-range for these change-point analyses, we note the somewhat limited power of the present sample and the cross-sectional design of this study as limitations. Still, the transition between childhood and adolescence that we have identified tentatively

Table 6
Age-dependent changes in functional connectivity (FC) with the bilateral centromedial subregion.

Structure	BA	Voxels (mm^3)	Peak coordinates (x, y, z)	Direction of change with increasing age	Child FC	Adult FC
(*R) Amygdala-L,R		23,803	17, −10, −17	↓	+	+
*Red nucleus-L,R						
*Culmen-L,R						
*Parahippocampal gyrus-L,R	34					
Posterior cingulate-L,R	30					
(*L) Thalamus-L,R						
Globus pallidus/putamen-L,R		11,648	45, 10, −19	↓	+	+
Superior temporal gyrus/sulcus-R	38, 41					
*Insula-R	13					
Claustrum-R						
*Dorsolateral superior frontal gyrus-L		11,577	−4, 49, 1	↑	No	+
Medial frontal gyrus-L,R	10					
Ventral anterior cingulate gyrus-L,R	10, 32					
	32, 24					

Table 7
Age-controlled functional connectivity with the bilateral superficial subregion.

Structure	BA	Voxels (mm^3)	Peak coordinates (x, y, z)
Positive connectivity			
Uncus-L,R		85,524	−14, −5, −13
Amygdala-L,R			
Hippocampus-L,R			
Parahippocampal gyrus-L,R			
Fusiform gyrus-L,R	36, 37		
Thalamus-L,R			
Globus pallidus/putamen-L,R			
Ventral superior-temporal gyrus-L,R	38, 41 13		
Insula-L,R			
Claustrum-L,R			
Caudate head-L,R			
Negative connectivity			
Cerebellum-L,R		69,812	31, −75, 39
Lingual gyrus-L,R	18		
Cuneus-L,R	17, 18, 19		
Middle temporal gyrus-L,R			
Posterior cingulate-R	31, 23		
Precuneus-L,R	7		
Angular gyrus-L,R			
Inferior parietal lobe-L,R	40		
Dorsal cingulate gyrus-L,R	23, 24, 31		
Precentral gyrus-R	6	24,391	24, 57, 19
Dorsal medial frontal gyrus-R	6, 8, 9		
Superior frontal gyrus-R	8		
Dorso-lateral middle frontal gyrus-R	6, 8, 9, 10		
Precentral gyrus-L	6	15,975	−25, 56, 11
Medial frontal gyrus-L	8		
Superior frontal gyrus-L	8		
Dorso-lateral middle frontal gyrus-L	6, 8, 9		

marks a specific, significant point of change in the nature of functional connections between the amygdala and the cortex. Future studies with greater power from larger samples of developing youth and longitudinal designs should be pursued to better quantify or corroborate this initial report of developmental change-points in connectivity.

Notably, several potential mechanisms may underlie these functional network developmental shifts. First, changes in pubertal hormone dynamics occurring around this time may play a mechanistic role in this connectivity shift, although we did not find that scores on our pubertal questionnaire measure were related to these network changes. It is possible that a more sensitive pubertal measure (e.g. hormonal levels in blood samples) could detect such a relation. It is also possible that the social and environmental changes that also mark this transition between childhood and adolescence (e.g. moving to middle school, increased peer socialization and increased time spent away from the family) may elicit these connectivity shifts within the brain. Moreover, a shift in anatomical connectivity metrics across the whole brain has also recently been identified during the late childhood to early adolescence period suggesting that anatomical network re-organization occurs during these years that may interact with the amygdala's functional network shifts we have observed (Khundrakpam et al., 2013). Future studies targeting these developmental shifts in pubertal and social contexts that combine functional and structural network approaches could distinguish between the roles of these potential mechanisms.

Given previous evidence that the presence of resting-state connectivity reflects stable network connections, the absence of amygdala–cortical connectivity at rest before adolescence suggests that childhood may be a period of unstable, dynamic amygdala–cortical connectivity that then stabilizes gradually during adolescence. Support for such an interpretation comes from a recent developmental clinical case study in which functional networks known to be unstable were also marked by the absence or significant reduction in coupling at rest, and typical resting coupling was recovered only by surgical intervention stabilizing these networks (Pizoli et al., 2011). Notably, task based studies have shown late development of amygdala–prefrontal functional connections (Perlman and Pelphrey, 2011), and we have previously shown that emotional stimuli can elicit an immature amygdala–mPFC connectivity phenotype during childhood, demonstrating that there is not simply a complete absence of functional coupling early in development for this network (Gee et al., 2013). These resting-state results suggest the possibility that childhood demarcates an important, malleable period in the construction of the amygdala–cortical networks, perhaps accompanied by increased sensitivity to environmental influences, whose functional significance for behaviors and interventions merits further investigation.

Further empirical investigation is needed to determine how the accompanying age-related segregation of amygdala–cortical functional connections into both positive and negative coupling patterns that we observed may be interpreted. The increase in amygdala–mPFC functional connectivity with age is consistent with graph theory approaches generalizing across functional networks that have characterized the development of positive resting-state connectivity as shifts from anatomically-local to more-distant but functionally relevant cortical connections as coupling within a network become better integrated (Fair et al., 2009; Supekar et al., 2009; Uddin et al., 2010). However, the meaning of shifts to negative coupling across development that

Table 8
Age-dependent changes in functional connectivity (FC) with the bilateral superficial subregion.

Structure	BA	Voxels (mm^3)	Peak coordinates (x, y, z)	Direction of change with increasing age	Child FC	Adult FC
Cerebellum-L,R		8623	21, −38, −9	↓	No	−
Parahippocampal gyrus-R						
Lingual gyrus-R	18					
*Middle occipital gyrus-R	18					
Posterior cingulate gyrus-R	30					
*Thalamus-L,R		30,015	21, 11, −5	↓	+	No
*Globus pallidus-R						
Putamen-R						
*Superior temporal sulcus/gyrus-R	22, 38, 42, 41					
*Inferior parietal lobe-R	40					
Post-central gyrus-R	2, 3					
Pre-central gyrus-R	4, 6					
*Insula-R	13					
*Caudate-R						
Dorso-lateral inferior frontal gyrus-R	44, 47					
Medial frontal gyrus	10, 32	7888	3, 55, −1	↑	No	+
Ventral anterior cingulate cortex	32, 24					

* Indicates regions where superficial connectivity is orthogonal to laterobasal and centromedial subregion connectivity (masking approach).

Table 9
Orthogonal (contrast approach) age-dependent changes in functional connectivity (FC) with the laterobasal amygdala subregion.

Structure	BA	Voxels (mm^3)	Peak coordinates (x, y, z)	Direction of change with increasing age
Thalamus		57,830	1, −18, −2	↑
Lentiform nucleus-L,R				
Parahippocampal gyrus-R	34			
Fusiform gyrus-L,R	36, 37			
Inferior occipital gyrus-L,R				
Middle occipital gyrus-L,R	18			
Culmen-L,R				
Cerebellum-L,R				
Cuneus-L	17, 18, 19	34,799	1, −34, 14	↓
Precuneus-L,R	7			
Posterior cingulate gyrus-L,R	30, 23			
Insula-L	13			
Superior temporal gyrus-L	36, 37			
Middle temporal gyrus-L				

we identified for both the insular/STS/G and posterior cingulate/parahippocampal regions is presently unresolved. While these developmental graph theory approaches have yet to be robustly applied to negative connectivity, developmental shifts from positive to negative resting-state connectivity have recently been reported for another functional network (Chai et al., 2014), and a recent sophisticated simulation of neural activity patterns at rest coupled with empirically-measured structural connectivity suggest that such negative connectivity is biologically meaningful and may represent complex patterns between regions within a network (Cabral et al., 2011). The segregation into positive and negatively valenced connectivity with the amygdala may thus reflect increasing sophistication of functional coupling between the regions as the network matures and merits future exploration.

It is possible that the age-related change in patterns of amygdala connectivity across these three cortical regions reflects a rostral shift in the appearance of positive coupling across the cortex with age. That is, we observed positive amygdala coupling with subcortical regions present by early childhood, in the insula/STS region during childhood, and positive PFC–amygdala coupling with mPFC later during adolescence and adulthood. The pattern observed across these regions is in line with previous work that has established a developmental rostral shift from the posterior to inferior direction in cortical structural ontogeny and in the development of synaptic density and dendritic length, grey matter volume, and white matter volume (Gogtay et al., 2004; Huttenlocher, 1990; Sowell et al., 2007). The rostral shift in positive

Table 10
Orthogonal (contrast approach) age-dependent changes in functional connectivity (FC) with the centromedial amygdala subregion.

Structure	BA	Voxels (mm^3)	Peak coordinates (x, y, z)	Direction of change with increasing age
Cerebellum-LR		25,274	22, −82, 32	↓
Culmen-L,R				
Fusiform gyrus-L	36, 37			
Lingual gyrus-L,R	18			
Inferior occipital gyrus-L,R				
Middle occipital gyrus-L,R	18			
Cuneus-R	17, 18, 19			
Posterior cingulate gyrus-L	30, 31, 23	11,104	−3, −51, 60	↑
Precuneus-L	7			
Postcentral gyrus-L	2, 3			
Precentral gyrus-L	4, 6			
Cingulate gyrus-L	24, 31			
Posterior cingulate gyrus-L	30, 31, 23	8209	−3, −76, 29	↑
Cuneus-L	17, 18, 19			
Precuneus-L	7			

Table 11
Orthogonal (contrast approach) age-dependent changes in functional connectivity (FC) with the superficial amygdala subregion.

Structure	BA	Voxels (mm^3)	Peak coordinates (x, y, z)	Direction of change with increasing age
Cerebellum		41,645	−51, −59, −3	↓
Cuneus-L,R	17, 18, 19			
Fusiform gyrus-L,R	36, 37			
Inferior occipital gyrus-R				
Middle occipital gyrus-L,R	18			
Lingual gyrus-L,R	18			
Posterior cingulate gyrus-R	30, 31, 23	20,656	−6, −78, 29	↑
Precuneus-L,R	7			
Cuneus-L	17, 18, 19			
Cingulate gyrus-L	24, 31			
Thalamus-L,R		18,968	1, −18, −2	↓
Lentiform nucleus-L				
Caudate-R				
Posterior cingulate-R	30, 31, 23	11,565	1, −30, 17	↑
Middle temporal gyrus-R	38, 41			
Cingulate gyrus-R	24, 31			
Insula-R				
Caudate-R				

coupling across the cortical regions we identified may reflect these developmental trends in the underlying neurobiology, although the interaction between these processes of neural network maturation and the resulting resting-state functional coupling requires further empirical investigation.

Extending prior work identifying connectivity with BL and CM amygdala subregions, we observed developmental differences in whole-brain functional coupling between anatomical subregions of LB, CM, and SF amygdala, in accord with preliminary imaging studies that distinguish mature functions and networks for these subregions in adult humans (Ball et al., 2007; Davis et al., 2010; Roy et al., 2009). In this study, the developmentally-constant functional coupling patterns unique to each subregion were largely consistent with the mature patterns previously identified among adults (Qin et al., 2012; Roy et al., 2009). As a recent report comparing LB and CM functional connections to several target networks in late childhood found reduced segregation of connectivity across these two subregions compared to adults (Qin et al., 2012), we sought to characterize the age-related patterns of connectivity segregation from early childhood through adulthood for the LB, CM, and SF subregions. Importantly, we observed age-related patterns of coupling changes unique to each subregion with respect to both connectivity valence and target locations. Specifically, the LB subregion became increasingly negatively coupled with broad dorsal-parietal and posterior regions across development, supporting the widespread negative coupling with these areas observed among adults at rest (Roy et al., 2009). The CM subregion became positively coupled with anterior and dorsal regions, consistent with its role in cortical attention (Davis et al., 1997), while the SF subregion showed a loss of diffuse positive coupling around ventral/limbic structures, supporting animal literature suggesting that the SF is involved specifically in affective processing (Price, 2003). That is, with increasing age, the LB functional network spread broadly across the cortex, the CM became coupled with specific new target regions, and a diffuse SF ventral network became focused specifically to limbic regions. As with the connectivity changes observed for the whole amygdala, these subregions' patterns of connectivity change occurred across the extensive developmental period from early childhood to adulthood.

Importantly, a conjunction analysis revealed that developmental changes in coupling between all three subregions also converged for several target regions, suggesting that integration across subregion networks occurs as well as segregation during development. Notably, the only region of convergence for which the LB, CM, and SB subregions all became increasingly positively coupled across development was the mPFC region. This coupling reveals that amygdala–mPFC

connections are particularly robust and pervasive across amygdala subregions, supporting the idea that mPFC coupling is central to amygdala function, since coupling is observed for all subregions despite their distinct functionalities (Ball et al., 2007; Davis et al., 2010; Kim et al., 2011b). Lastly, the remaining insula, STS, posterior cingulate, and parahippocampal regions of convergence were characterized by shifts to opposite coupling valences across the subregions (negative coupling with the LB and positive coupling with the SF and CM across development). Consistent opposing patterns of coupling noted in adults thus appear to show protracted developmental changes as amygdala functional networks are refined across childhood and adolescence (Roy et al., 2009; Tottenham and Sheridan, 2009). Further task-based assessment of subregion functions should be performed to determine how the development of opposing coupling patterns at rest inform the development of opposing functional roles across subregions, and can help delineate the unique functional contributions of each subregion to specific affective and cognitive processes that emerge across development.

Importantly, future longitudinal assessments of amygdala–cortical networks as well as future studies distinguishing between amygdala anatomical subregions are necessary to build on these results and robustly characterize true developmental trajectories of functional coupling with the amygdala in terms of duration and precise timing of coupling changes, which cross-sectional designs are unable to address. Additionally, the functional connectivity methods we employed in this study provide correlational relations only between regions, and therefore cannot detail causal influences in the development of these networks. Effective connectivity approaches assessing directionality could address these very pertinent questions in functional connectivity development in the future. It should also be noted that these resting-state data were collected at the end of scanning sessions for all participants, as some regions of interest have shown task-influenced alterations in another resting-state measure (Wang et al., 2012), although other studies have not found such ordering effects on amygdala resting-state connectivity (e.g. Kim et al., 2011b) and the concordance between our age-constant analyses and the findings of Roy et al. (2009) whose study was conducted without tasks beforehand suggests that such ordering limitations have not insidiously impacted our data.

In conclusion, we have shown that the extent and nature of developmental changes in resting functional coupling with the amygdala vary across the brain with consequences for our search to understand how the stabilization of networks occurs across development. Functional connectivity between the amygdala and several cortical regions displayed lengthy and complex trajectories of change. The period between 4 and 10 years old was characterized by a different connectivity quality as compared to older ages, suggesting that childhood may represent a unique period of potential malleability in amygdala–cortical connectivity development and revealing the transition from childhood to adolescence as an important point of change for this amygdala–cortical functional network underlying complex emotion processing and regulation. In contrast, functional coupling between the amygdala and limbic, subcortical regions appears to undergo an early and rapid stabilization largely before childhood to support affect generation processes (although the noted exception is the parahippocampal gyrus, which demonstrated changes in coupling with the amygdala across development). Thus, the timing when amygdala functional connections may be malleable and sensitive to environmental influences depends on the location of the coupling region within the brain. Furthermore, each of the amygdala anatomical subregions demonstrated unique developmental changes in coupling that were differentiated across subregions both by the patterns of network segregation and the coupling valence with several regions of convergence that occurred across development. Together, these results demonstrate that extensive, specific changes in amygdala functional coupling from early childhood through adolescence are required to achieve mature, stable functional networks in adulthood.

Funding

This work was supported by the National Institute of Mental Health (R01MH091864 to N.T.) and the National Science Foundation (DGE-1144087 to L.J.G-D).

Conflict of interest

The authors declare no competing financial interests.

Appendix A. Supplementary data

Supplementary data to this article can be found online at http://dx.doi.org/10.1016/j.neuroimage.2014.03.038.

References

Adolphs, R., Spezio, M., 2006. Role of the amygdala in processing visual social stimuli. Prog. Brain Res. 156, 363–378.
Amaral, D.G., Price, J.L., Pitkanen, A., Carmichael, S.T., 1992. Anatomical organization of the primate amygdaloid complex. In: Aggleton, J.P. (Ed.), The Amygdala: Neurobiological Aspects of Emotion, Memory, and Mental Dysfunction. Wiley-Liss, New York, pp. 1–66.
Amunts, K., Kedo, O., Kindler, M., Pieperhoff, P., Mohlberg, H., Shah, N.J., Habel, U., Schneider, F., Zilles, K., 2005. Cytoarchitectonic mapping of the human amygdala, hippocampal region and entorhinal cortex: intersubject variability and probability maps. Anat. Embryol. 210, 343–352.
Anand, A., Li, Y., Wang, Y., Wu, J., Gao, S., Bukhari, L., Mathews, V.P., Kalnin, A., Lowe, M.J., 2005. Activity and connectivity of brain mood regulating circuit in depression: a functional magnetic resonance study. Biol. Psychiatry 57, 1079–1088.
Ball, T., Rahm, B., Eickhoff, S.B., Schulze-Bonhage, A., Speck, O., Mutschler, I., 2007. Response properties of human amygdala subregions: evidence based on functional MRI combined with probabilistic anatomical maps. PLoS One 2, e307.
Banks, S.J., Eddy, K.T., Angstadt, M., Nathan, P.J., Phan, K.L., 2007. Amygdala-frontal connectivity during emotion regulation. Soc. Cogn. Affect. Neurosci. 2, 303–312.
Baseler, H.A., Harris, R.J., Young, A.W., Andrews, T.J., 2012. Neural responses to expression and gaze in the posterior superior temporal sulcus interact with facial identity. Cereb. Cortex 24, 737–744.
Berking, M., Wupperman, P., 2012. Emotion regulation and mental health: recent findings, current challenges, and future directions. Curr. Opin. Psychiatry 25, 128–134.
Bunge, S.A., Dudukovic, N.M., Thomason, M.E., Vaidya, C.J., Gabrielli, J.D., 2002. Immature frontal lobe contributions to cognitive control in children: evidence from fMRI. Neuron 33, 301–311.
Cabral, J., Hugues, E., Sporns, O., Deco, G., 2011. Role of local network oscillations in resting-state functional connectivity. NeuroImage 57, 130–139.
Casey, B.J., Trainor, R., Giedd, J., Vauss, Y., Vaituzis, C.K., Hamburger, S., Kozuch, P., Rapoport, J.L., 1997. The role of the anterior cingulate in automatic and controlled processes: a developmental neuroanatomical study. Dev. Psychobiol. 30, 61–69.
Casey, B.J., Giedd, J.N., Thomas, K.M., 2000. Structural and functional brain development and its relation to cognitive development. Biol. Psychol. 54, 241–257.
Chai, X.J., Ofen, N., Gabrieli, J.D.E., Whitfield-Gabrieli, S., 2014. Selective development of anticorrelated networks in the intrinsic functional organization of the human brain. J. Cogn. Neurosci. 26, 501–513.
Chang, C., Glover, G.H., 2009. Effects of model-based physiological noise correction on default mode network anti-correlations and correlations. NeuroImage 47, 1448–1459.
Chen, G., Chen, G., Xie, C., Ward, B.D., Li, W., Antuono, P., Li, S.J., 2012. A method to determine the necessity for global signal regression in resting-state fMRI studies. Magn. Reson. Med. 68, 1828–1835.
Cisler, J.M., Olatunji, B.O., 2012. Emotion regulation and anxiety disorders. Curr. Psychiatry Rep. 14, 182–187.
Cox, R.W., 1996. AFNI: software for analysis and visualization of functional magnetic resonance neuroimages. Comput. Biomed. Res. 29, 162–173.
Das, P., Kemp, A.H., Flynn, G., Harris, A.W., Liddell, B.J., Whitford, T.J., Peduto, A., Gordon, E., Williams, L.M., 2007. Functional disconnections in the direct and indirect amygdala pathways for fear processing in schizophrenia. Schizophr. Res. 90, 284–294.
Davis, K.D., Talor, S.J., Crawley, A.P., Wood, M.L., Mikulis, D.J., 1997. Functional MRI of pain- and attention-related activations in the human cingulate cortex. J. Neurophysiol. 77, 3370–3380.
Davis, F.C., Johnstone, T., Mazzulla, E.C., Oler, J.A., Whalen, P.J., 2010. Regional response differences across the human amygdaloid complex during social conditioning. Cereb. Cortex 20, 612–621.
Etkin, A., Egner, T., Peraza, D.M., Kandel, E.R., Hirsch, J., 2006. Resolving emotional conflict: a role for the rostral anterior cingulate cortex in modulating activity in the amygdala. Neuron 51, 871–882.
Etkin, A., Egner, T., Kalisch, R., 2011. Emotional processing in anterior cingulate and medial prefrontal cortex. Trends Cogn. Sci. 15, 85–93.
Fair, D.A., Cohen, A.L., Power, J.D., Dosenbach, N.U.F., Church, J.A., Miezin, F.M., Schlaggar, B.L., Petersen, S.E., 2009. Functional brain networks develop from a "local to distributed" organization. PLoS Comput. Biol. 5, e1000381.
Fisher, P.M., Meltzer, C.C., Price, J.C., Coleman, R.L., Ziolko, S.K., Becker, C., Moses-Kolko, E.L., Berga, S.L., Hariri, A.R., 2009. Medial prefrontal cortex 5-HT(2A) density is correlated

with amygdala reactivity, response habituation, and functional coupling. Cereb. Cortex 19, 2499–2507.
Fox, M.D., Zhang, D., Snyder, A.Z., Raichle, M.E., 2009. The global signal and observed anticorrelated resting state brain networks. J. Neurophysiol. 101, 3270–3283.
Gee, D.G., Humphreys, K.L., Flannery, J., Goff, B., Telzer, E.H., Shapiro, M., Hare, T.A., Bookheimer, S.Y., Tottenham, N., 2013. A developmental shift from positive to negative connectivity in human amygdala–prefrontal circuitry. J. Neurosci. 33, 4584–4593.
Giedd, J.N., Vaituzis, A.C., Hamburger, S.D., Lange, N., Rajapakse, J.C., Kaysen, D., Vauss, Y.C., Rapoport, J.L., 1996. Quantitative MRI of the temporal lobe, amygdala, and hippocampus in normal human development: ages 4–18 years. J. Comp. Neurol. 366, 223–230.
Gilmore, J.H., Shi, F., Woolson, S.L., Knickmeyer, R.C., Short, S.J., Lin, W., Zhu, H., Hamer, R. M., Styner, M., Shen, D., 2012. Longitudinal development of cortical and subcortical gray matter from birth to 2 years. Cereb. Cortex 22, 2478–2485.
Gogtay, N., Giedd, J.N., Lusk, L., Hayashi, K.M., Greenstein, D., Vaituzis, A.C., Nugent III, T.F., Herman, D.H., Clasen, L.S., Toga, A.W., Rapoport, J.L., Thompson, P.M., 2004. Dynamic mapping of human cortical development during childhood through early adulthood. Proc. Natl. Acad. Sci. U. S. A. 101, 8174–8179.
Goldin, P.R., McRae, K., Ramel, W., Gross, J.J., 2008. The neural bases of emotion regulation: reappraisal and suppression of negative emotion. Biol. Psychiatry 63, 577–586.
Hallquist, M.N., Hwang, K., Luna, B., 2013. The nuisance of nuisance regression: spectral misspecification in a common approach to resting-state fMRI preprocessing reintroduces noise and obscures functional connectivity. NeuroImage 82, 208–225.
Hampson, M., Driesen, N., Roth, J.K., Gore, J.C., Constable, R.T., 2010. Functional connectivity between task-positive and task-negative brain areas and its relation to working memory performance. Magn. Reson. Imaging 28, 1051–1057.
Hare, T.A., Tottenham, N., Galvan, A., Voss, H.U., Glover, G.H., Casey, B.J., 2008. Biological substrates of emotional reactivity and regulation in adolescence during an emotional go–nogo task. Biol. Psychiatry 63, 927–934.
Hariri, A.R., Mattay, V.S., Tessitore, A., Fera, F., Weinberger, D.R., James, W., 2003. Neocortical modulation of the amygdala response to fearful stimuli. Biol. Psychiatry 53, 494–501.
He, H., Liu, T.T., 2012. A geometric view of global signal confounds in resting-state functional MRI. NeuroImage 59, 2339–2348.
Henry, J.D., Rendell, P.G., Green, M.J., McDonald, S., O'Donnell, M., 2008. Emotion regulation in schizophrenia: affective, social, and clinical correlates of suppression and reappraisal. J. Abnorm. Psychol. 117, 473–478.
Huttenlocher, P.R., 1990. Morphometric study of human cerebral cortex development. Neuropsychologia 28, 517–527.
Khundrakpam, B.S., Reid, A., Brauer, J., Carbonell, F., Lewis, J., Ameis, S., et al., 2013. Developmental changes in organization of structural brain networks. Cereb. Cortex 23, 2072–2085.
Killgore, W.D., Yurgelun-Todd, D.A., 2004. Sex-related developmental differences in the lateralized activation of the prefrontal cortex and amygdala during perception of facial affect. Percept. Mot. Skills 99, 371–391.
Kim, M.J., Loucks, R.A., Palmer, A.L., Brown, A.C., Solomon, K.M., Marchante, A.N., Whalen, P.J., 2011a. The structural and functional connectivity of the amygdala: from normal emotion to pathological anxiety. Behav. Brain Res. 223, 403–410.
Kim, M.J., Gee, D.G., Loucks, R.A., Davis, F.C., Whalen, P.J., 2011b. Anxiety dissociates dorsal and ventral medial prefrontal cortex functional connectivity with the amygdala at rest. Cereb. Cortex 21, 1667–1673.
LeDoux, J., 2003. The emotional brain, fear, and the amygdala. Cell. Mol. Neurobiol. 23, 727–738.
Lee, H., Heller, A.S., van Reekum, C.M., Nelson, B., Davidson, R.J., 2012. Amygdala–prefrontal coupling underlies individual differences in emotion regulation. NeuroImage 62, 1575–1581.
Linnman, C., Zeidan, M.A., Furtak, S.C., Pitman, R.K., Quirk, G.J., Milad, M.R., 2012. Resting amygdala and medial prefrontal metabolism predicts functional activation of the fear extinction circuit. Am. J. Psychiatry 169, 415–423.
Lou, H.C., Luber, B., Crupain, M., Keenan, J.P., Nowak, M., Kjaer, T.W., Sackeim, H.A., Lisanby, S.H., 2004. Parietal cortex and representation of the mental self. Proc. Natl. Acad. Sci. U. S. A. 101, 6827–6832.
Luna, B., Thulborn, K.R., Munoz, D.P., Merriam, E.P., Garver, K.E., Minshew, N.J., Keshavan, M.S., Genovese, C.R., Eddy, W.F., Sweeney, J.A., 2001. Maturation of widely distributed brain function subserves cognitive development. NeuroImage 13, 786–793.
Maddock, R.J., Garrett, A.S., Buonocore, M.H., 2003. Posterior cingulate cortex activation by emotional words: fMRI evidence from a valence decision task. Hum. Brain Mapp. 18, 30–41.
McRae, K., Gross, J.J., Weber, J., Robertson, E.R., Sokol-Hessner, P., Ray, R.D., Gabrieli, J.D., Ochsner, K.N., 2012. The development of emotion regulation: an fMRI study of cognitive reappraisal in children, adolescents and young adults. Soc. Cogn. Affect. Neurosci. 7, 11–22.
Murphy, K., Birn, R.M., Handwerker, D.A., Jones, T.B., Bandettini, P.A., 2009. The impact of global signal regression on resting state correlations: are anti-correlated networks introduced? NeuroImage 44, 893–905.
Ochsner, K.N., Silvers, J.A., Buhle, J.T., 2012. Functional imaging studies of emotion regulation: a synthetic review and evolving model of the cognitive control of emotion. Ann. N. Y. Acad. Sci. 1251, E1–E24.
Perlman, S.B., Pelphrey, K.A., 2011. Developing connections for affective regulation: age-related changes in emotional brain connectivity. J. Exp. Child Psychol. 108, 607–620.
Pessoa, L., Adolphs, R., 2010. Emotion processing and the amygdala: from a "low road" to "many roads" of evaluating biological significance. Nat. Rev. Neurosci. 11, 773–783.
Petersen, A.C., Crockett, L., Richards, M., Boxer, A., 1988. A self-report measure of pubertal status: reliability, validity, and initial norms. J. Youth Adolesc. 17, 117–133.
Phan, K.L., Fitzgerald, D.A., Nathan, P.J., Moore, G.J., Uhde, T.W., Tancer, M.E., 2005. Neural substrates for voluntary suppression of negative affect: a functional magnetic resonance imaging study. Biol. Psychiatry 57, 210–219.
Phelps, E.A., O'Connor, K.J., Gatenby, J.C., Gore, J.C., Grillon, C., Davis, M., 2001. Activation of the left amygdala to a cognitive representation of fear. Nat. Neurosci. 4, 437–441.
Phillips, M.L., Drevets, W.C., Rauch, S.L., Lane, R., 2003. Neurobiology of emotion perception I: the neural basis of normal emotion perception. Biol. Psychiatry 54, 504–514.
Pitkänen, A., 2000. Connectivity of the rat amygdaloid complex. The amygdala: a functional analysis. 2, 31–115.
Pizoli, C.E., Shah, M.N., Snyder, A.Z., Shimony, J.S., Limbrick, D.D., Raichle, M.E., Schlaggar, B.L., Smyth, M.D., 2011. Resting-state activity in development and maintenance of normal brain function. Proc. Natl. Acad. Sci. U. S. A. 108, 11638–11643.
Power, J.D., Barnes, K.A., Snyder, A.Z., Schlaggar, B.L., Petersen, S.E., 2012. Spurious but systematic correlations in functional connectivity MRI networks arise from subject motion. NeuroImage 59, 2142–2154.
Price, J.L., 2003. Comparative aspects of amygdala connectivity. Ann. N. Y. Acad. Sci. 985, 50–58.
Qin, S., Young, C.B., Supekar, K., Uddin, L.Q., Menon, V., 2012. Immature integration and segregation of emotion-related brain circuitry in young children. Proc. Natl. Acad. Sci. U. S. A. 109, 7941–7946.
Raichle, M.E., 2010. Two views of brain function. Trends Cogn. Sci. 14, 180–190.
Roy, A.K., Shehzad, Z., Margulies, D.S., Kelly, A.M., Uddin, L.Q., Gotimer, K., Biswal, B.B., Castellanos, F.X., Milham, M.P., 2009. Functional connectivity of the human amygdala using resting state fMRI. NeuroImage 45, 614–626.
Saad, Z.S., Gotts, S.J., Murphy, K., Chen, G., Jo, H.J., Martin, A., Cox, R.W., 2012. Trouble at rest: how correlation patterns and group differences become distorted after global signal regression. Brain Connect. 2, 25–32.
Sarkheil, P., Goebel, R., Schneider, F., Mathiak, K., 2012. Emotion unfolded by motion: a role for parietal lobe in decoding dynamic facial expressions. Soc. Cogn. Affect. Neurosci. 8, 950–957.
Satterthwaite, T.D., Wolf, D.H., Loughead, J., Ruparel, K., Elliott, M.A., Hakonarson, H., Gur, R.C., Gur, R.E., 2012. Impact of in-scanner head motion on multiple measures of functional connectivity: relevance for studies of neurodevelopment in youth. NeuroImage 60, 623–632.
Sowell, E.R., Trauner, D.A., Gamst, A., Jernigan, T.L., 2007. Development of cortical and subcortical brain structures in childhood and adolescence: a structural MRI study. Dev. Med. Child Neurol. 44, 4–16.
Sporns, O., Zwi, J.D., 2004. The small world of the cerebral cortex. Neuroinformatics 2, 145–162.
Supekar, K., Musen, M., Menon, V., 2009. Development of large-scale functional brain networks in children. PLoS Biol. 7, e1000157.
Swartz, J.R., Carrasco, M., Wiggins, J.L., Thomason, M.E., Monk, C.S., 2014. Age-related changes in the structure and function of prefrontal cortex–amygdala circuitry in children and adolescents: a multimodal imaging study. NeuroImage 86, 212–220.
Talairach, J., Tournoux, P., 1988. Co-planar stereotaxic atlas of the human brain. Theime, Germany, Stuttgart.
Thomas, K.M., Drevets, W.C., Whalen, P.J., Eccard, C.H., Dahl, R.E., Ryan, N.D., Casey, B.J., 2001. Amygdala response to facial expressions in children and adults. Biol. Psychiatry 49, 309–316.
Tomasi, D., Wang, G.J., Volkow, N.D., 2013. Energetic cost of brain functional connectivity. Proc. Natl. Acad. Sci. U. S. A. 110, 13642–13647.
Tottenham, N., Sheridan, M.A., 2009. A review of adversity, the amygdala and the hippocampus: a consideration of developmental timing. Front. Hum. Neurosci. 3, 68.
Uddin, L.Q., Supekar, K., Menon, V., 2010. Typical and atypical development of functional human brain networks: insights from resting-state FMRI. Front. Syst. Neurosci. 4, 21.
Ulfig, N., Setzer, M., Bohl, J., 2003. Ontogeny of the human amygdala. Ann. N. Y. Acad. Sci. 985, 22–33.
van den Heuvel, M.P., Hulshoff Pol, H.E., 2010. Exploring the brain network: a review on resting-state fMRI functional connectivity. Eur. Neuropsychopharmacol. 20, 519–534.
Van Dijk, K.R., Hedden, T., Venkataraman, A., Evans, K.C., Lazar, S.W., Buckner, R.L., 2010. Intrinsic functional connectivity as a tool for human connectomics: theory, properties, and optimization. J. Neurophysiol. 103, 297–321.
Van Dijk, K.R., Sabuncu, M.R., Buckner, R.L., 2012. The influence of head motion on intrinsic functional connectivity MRI. NeuroImage 59, 431–438.
Wang, F., Kalmar, J.H., He, Y., Jackowski, M., Chepenik, L.G., Edmiston, E.E., Tie, K., Gong, G., Shah, M.P., Jones, M., Uderman, J., Constable, R.T., Blumberg, H.P., 2009. Functional and structural connectivity between the perigenual anterior cingulate and amygdala in bipolar disorder. Biol. Psychiatry 66, 516–521.
Wang, D.-Y., Han, X.-J., Li, S.-F., Liu, D.-Q., Yan, C.-G., Zuo, X.-N., Zhu, C.-Z., He, Y., Kiviniemi, V., Zang, Y.-F., 2012. Effects of Apolipoprotein E genotype on the off-line memory consolidation. PLoS One 7, e51617.
Weissenbacher, A., Kasess, C., Gerstl, F., Lanzenberger, R., Moser, E., Windischberger, C., 2009. Correlations and anticorrelations in resting-state functional connectivity MRI: a quantitative comparison of preprocessing strategies. NeuroImage 47, 1408–1416.
Yan, C.G., Cheung, B., Kelly, C., Colcombe, S., Craddock, R.C., Di Martino, A., Li, Q., Zuo, X.N., Castellanos, F.X., Milham, M.P., 2013. A comprehensive assessment of regional variation in the impact of head micromovements on functional connectomics. NeuroImage 76, 183–201.
Zhang, S., Li, C.R., 2012. Functional connectivity mapping of the human precuneus by resting state fMRI. NeuroImage 59, 3548–3562.
Zhang, S., Li, C.-S.R., 2013. Functional clustering of the human inferior parietal lobule by whole brain connectivity mapping of resting state fMRI signals. Brain Connect. http://dx.doi.org/10.1089/brain.2013.0191.
Zhang, S., Hu, S., Chao, H.H., Ide, J.S., Luo, X., Farr, O.M., Li, C.-S.R., 2013. Ventromedial prefrontal cortex and the regulation of physiological arousal. Soc. Cogn. Affect. Neurosci. http://dx.doi.org/10.1093/scan/nst064.